KINETICS OF CARRIER-MEDIATED ION TRANSPORT IN TWO NEW TYPES OF SOLVENT-FREE LIPID BILAYERS

JEAN-YVES LAPOINTE AND RAYNALD LAPRADE
Département de Physique, Université de Montréal, Montréal, Québec, Canada

ABSTRACT In contrast with the usual glyceryl-monooleate/decane (GMO-D) bilayer lipid membranes, new membranes, formed from a mixture of GMO in squalene (GMO-S) or from a mixture of GMO in triolein (GMO-T), seem to be almost solvent free. Our results from voltage-jump relaxation studies, using these "solvent-free" membranes with the homologue carriers, nonactin, monactin, dinactin, trinactin, and tetranactin, are compared with the corresponding ones for GMO-D membranes. With all homologues, solvent-free membranes show an increase of the free carrier translocation rate, k_s, by a factor of 2.5, a decrease in the dissociation rate constant of the complex, k_{Di}, by a factor of 1.5 and no significant change in its formation rate constant, k_{Ri}. However, the principal effect of the absence of solvent in these membranes is an increase by a factor of ~10 of the translocation rate constant for moving the complex across the membrane, k_{is}. This increase varies regularly from a factor of 7–15 with decreasing carrier size, and is always larger for GMO-T than for GMO-S membranes. These solvent-free effects are interpreted in terms of modifications of electrostatic and hydrophobic energy profiles in the membrane.

INTRODUCTION

The technique for the formation of lipid bilayer membranes (BLM) was originally introduced by Mueller et al. (1962). The BLM are generally made from a mixture of amphiphilic lipid and organic solvent (e.g., an alkane) on a small teflon aperture (1 mm diameter) between two aqueous phases. The organic solvent, which cannot interact very strongly with water, is there to satisfy the contact angle between the thin membrane and the Teflon aperture (White et al., 1976). However, in the final state an important amount of solvent (Henn and Thompson, 1968; Fettiplace et al., 1971; Pagano et al., 1972; White, 1977) remains in the BLM, thus questioning its use as a model for natural membranes.

Until 1978 the so-called "solvent-free" membranes were made exclusively with Montal's technique (Montal and Mueller, 1972). This is a rather difficult technique that gives very thin membranes (26 Å for GMO as compared with 49.5 Å for GMO/decane) but of small diameter (~0.2 mm). Moreover this technique requires conditioning of the septum with petroleum jelly, or chloroform, silicone, etc., which can eventually migrate into the membrane (Benz et al., 1975; White, 1978).

Recently, two new techniques have been introduced that allow one to obtain stable solvent-free membranes with large diameters (>1 mm) and with a thinness never reached before. White (1978), using a forming solution of GMO dispersed in squalene (GMO-S), has measured a specific capacitance of 0.7771 ± 0.0041 μF/cm^2 corresponding to a dielectric thickness of 25.1 Å. On the other hand, Waldbillig and Szabo (1979), using a forming solution of GMO in triglyceride (GMO-T) (a pure lipid solution), have measured a specific capacitance of 0.862 ± 0.015 μF/cm^2 corresponding to a dielectric thickness of 22.6 Å. In principle, if these two new techniques really give solvent-free membranes, both should have the same thickness. The fact that GMO-S and GMO-T membranes are indeed different will be confirmed by our observations.

In this work we will present voltage-jump relaxation studies with nonactin and its four homologues (monactin, dinactin, trinactin, and tetranactin) from which we will deduce their rate constants for NH_4^+ transport across GMO-S and GMO-T membranes. We will then compare these rate constants between the different homologues as well as between decane-containing (GMO-D) and solvent-free bilayers. Finally, we will analyze the observed systematic variations in terms of modifications of electrostatic and/or hydrophobic energy barriers. The values of the rate constants for GMO-D membranes will be taken from the work of Laprade et al. (1982).

THEORY

The transport model we will use is schematized in Fig. 1 and is the same as that used by Laprade et al. (1982). It corresponds to the widely accepted model for carrier-mediated ion transport utilized by Läuger and Stark (1970) and Stark et al. (1971). This model is essentially identical to that of Ciani (Ciani et al., 1973; Laprade et al., 1975) with the omission of the complex partition process. The notation used here is that of Hladky's recent review (Hladky, 1979*a*) which is a slightly modified version of that of Läuger and Stark (1970).

In this scheme, an ion i in the aqueous phase reacts at the interface with a carrier s^* in the membrane to form a complex is^* according to the following reaction

$$i + s^* \underset{k_{Di}}{\overset{k_{Ri}}{\rightleftharpoons}} is^* \qquad (1)$$

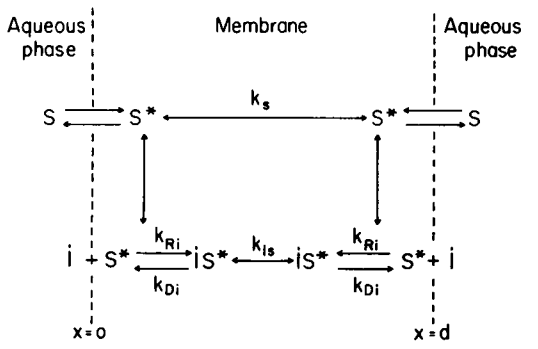

FIGURE 1 Schematic diagram of the processes involved in carrier-mediated ion transport. The symbols *i*, *s*, and *is* represent, respectively, an ion, a carrier, and a complex. We add a superscript * to the species that are in the membrane. See text for detailed discussion.

where k_{Ri} and k_{Di} are, respectively, the rate constants for formation and dissociation of the complex.

The free carrier s^* and the complex is^* in the membrane can jump from one side (') to the other (") and vice versa:

$$s^{*\prime} \xleftrightarrow{k_s} s^{*\prime\prime} \tag{2}$$

$$is^{*\prime} \underset{k''_{is}}{\overset{k'_{is}}{\rightleftharpoons}} is^{*\prime\prime} \tag{3}$$

where $k'_{is} = k''_{is} = k_{is}$ at zero applied voltage. In the present treatment, the translocation rate constant of the complex (k'_{is} or k''_{is}) is the only one that is considered to be voltage dependent. The implications of this assumption will be discussed in detail further on.

Time Dependence of the Electric Current

For such a system, it has been shown in an Eyring type of treatment (Stark et al., 1971; Laprade et al., 1975; Hladky, 1975) that the time course of the current after a voltage jump is given by

$$I(t) = I_\infty(1 + \alpha_1 e^{-t/\tau_1} + \alpha_2 e^{-t/\tau_2}) \tag{4}$$

where I_∞ is the steady-state or stationary current, which, for the case of a monovalent cation and a carrier added via the aqueous phase, is given by

$$I_\infty = Fd\gamma_s \frac{k_{Ri}}{k_{Di}} k_{is} \frac{c_s^a c_i}{[1 + Kc_i]} \frac{\sinh(u/2)}{[1 + A\cosh(u/2)]}. \tag{5}$$

α_1 and α_2 are the relaxation amplitudes, and τ_1 and τ_2 are the relaxation time constants, which are given by

$$1/\tau_1 = a - b \tag{6}$$

$$1/\tau_2 = a + b, \tag{7}$$

where

$$2a = 2\,k_{is}\cosh(u/2) + k_{Di} + 2\,k_s + k_{Ri}c_i \tag{8}$$

$$2b = [(2\,k_{is}\cosh(u/2) + k_{Di} - 2\,k_s - k_{Ri}c_i)^2 + 4\,k_{Ri}c_i\,k_{Di}]^{1/2} \tag{9}$$

$$\alpha_1 = \frac{A}{2}\cosh(u/2) + B \tag{10}$$

$$\alpha_2 = \frac{A}{2}\cosh(u/2) - B \tag{11}$$

$$B = \frac{\cosh(u/2)}{4b} \cdot \{A[k_{Ri}c_i + k_{Di} + 2\,k_s - 2\,k_{is}\cosh(u/2)] - 4\,k_{is}\} \tag{12}$$

$$\alpha_1 + \alpha_2 = A\cosh(u/2) = \alpha_T \tag{13}$$

$$A = \frac{k_{is}}{k_{Di}}\left(2 + \frac{k_{Ri}c_i}{k_s}\right) \tag{14}$$

$$u = \frac{FV}{RT}. \tag{15}$$

In the above expressions, F is the Faraday, d, the membrane thickness, c_s^a, the total aqueous carrier concentrations, K, the aqueous phase ion-carrier complexation constant, γ_s, the aqueous phase-membrane carrier partition coefficient, and V, the applied voltage.

Zero-Current Conductance

In the limit of low applied voltages and thus low currents, we obtain from Eq. 5 the so-called zero-current conductance (Szabo et al., 1969; Läuger and Stark, 1970)

$$G_0^a = \lim_{V\to 0}\frac{I_\infty}{V} = \frac{F^2 d\gamma_s}{2RT} k_{is} \frac{k_{Ri}c_s^a c_i}{k_{Di}(1 + Kc_i)(1 + A)} \tag{16}$$

where the superscript a refers to the carrier added to the aqueous phase.

MATERIALS AND METHODS

GMO-D black lipid membranes were formed from a 25 mg/ml solution of monoolein (GMO) in *n*-decane. GMO-D membranes were formed according to previously published methods (Szabo et al., 1969). GMO-T membranes were formed from a solution of GMO in triolein at a GMO mole fraction of 0.44. GMO-S membranes were formed from a 100 mg/ml dispersion of GMO in squalene. GMO was obtained from Sigma Chemical Co., St. Louis, MO, or Nu-Check Prep Inc., Elysian, MN; triolein from Nu-Check Prep Inc.; and squalene was kindly supplied by Bruce Enos from the University of California at Los Angeles who purified it by two successive passages through an alumina column (White, 1978).

The above GMO concentrations in triolein or squalene produced stable membranes. They are quite adequate to obtain solvent-free bilayers because, on the one hand, Waldbillig and Szabo (1979) showed no effect of GMO mole fraction on the thickness of GMO-T membranes in the range 0.1–0.9. On the other hand, the higher than usual GMO concentration that we have used in GMO-S membranes (White, 1978) assures even better that the membrane is free of solvent (Waldbillig and Szabo, 1978).

The same method was used to form both types of membranes. The forming solution was vigorously stirred with a small and clean magnetic rod before the membrane was formed. To minimize carrier adsorption on the Teflon walls, the membrane was formed on a Teflon disk separating two glass compartments that each contained 20 ml of aqueous solutions (Laprade et al., 1979). The diameter of the aperture in the Teflon disk was 0.6 mm, and we used a spatulalike tool of the same diameter to form the membrane (Waldbillig and Szabo, 1979). This tool, made from a glass pipet, is necessary because of the high viscosity of the forming solution, particularly in the case of GMO-T membranes.

The measurements were carried out at room temperature, which was kept constant at 22.5°C. Nonactin was a gift from Barbara Sterns of Squibb Corp., NY, and Hans Bickel of Ciba-Geigy Limited, Basle, Switzerland; monactin, dinactin, and trinactin were gifts from Hans Bickel, and tetranactin was a gift from W. Simon (Swiss Federal Institute of Technology, Zürich, Switzerland), and from K. Ando (Research Lab., Chugai Phaum. Co., Ltd., Tokyo, Japan.) Small volumes of stock ethanol solutions (10^{-5} – 10^{-3} M) were added to the aqueous phase, the final

aqueous ethanol concentration never exceeding 1%. The ammonium was used as a chloride. Ionic strength was kept constant at 1 M with LiCl.

The conductance measurements were performed as in previous studies (Szabo, et al., 1969; Laprade et al., 1975). For the relaxation studies, the voltage pulses of ~1 ms duration were supplied by a pulse generator with a rise time of 10 ns (Hewlett Packard Co., Böblingen, FRG, model 8005A). A wide-band amplifier (RCA Solid State, Somerville, NJ, model CA3040) with a constant open loop gain of 30–100 MHz was used as a current amplifier with feedback resistors of 5.4 or 22.4 kΩ; its output was amplified by a second CA3040 in an open loop configuration. A Biomation 805 dual time-base transient recorder (Cupertino, CA) was used as a buffer to an averager (Fabri-Tek Instruments Inc. Madison, WI, model 1072). Signal repetition rates varied around 200 Hz, and 1,024–8,196 samples were taken on the same membrane. The first 90% of the current decay was recorded with the first time base at a setting that allowed maximum resolution, and the last 10% with the second time base at a 10 times slower setting, thus allowing the decay to be totally completed by the end of the recording. The output of the averager corresponding to $[I(t) - I_\infty]$, where I_∞ is the steady-state current, was fed to a logarithmic amplifier, whose output was displayed on an x-y plotter. The time constant of the exponential decay could be read directly from lhe slope of the straight line on the x-y plotter, the intercept at $t = 0$ giving the difference between instantaneous and steady-state current. Obviously the relaxation current could be relied upon only after the capacitive transient, whose time constant for the smallest membranes was 200 ns. The procedure has allowed us to measure relaxations of small amplitudes and short-time constants with increased precision using lower carrier concentrations.

Numerical Methods

The analysis of the rate constants from the relaxation data that we use requires curve-fitting the theoretically predicted values (X_{theor}) of the amplitudes and time constants of relaxation to the experimentally measured ones (X_{exp}). Indeed, to obtain the values of the parameters k_{is}, k_s, k_{Ri}, and k_{Di} that would give the optimum fit between experimental quantities and predicted ones over the whole experimental range, we have used a least-square fit program on a digital computer. This program, starting with hand calculated initial guesses for the values of the parameters, varies them until it finds a minimum (in four dimensions) for the sum of $[(X_{exp} - X_{theor})/X_{exp}]^2$ for all points. In this procedure, it is the relative difference that is minimized, so that each point is then given the same importance. The values for the initial guesses are obtained through approximations of Eqs. 6–15 in the limit of low permeant ion concentration and low applied voltage. For additional information, the reader is referred to Laprade et al. (1982).

RESULTS

Relaxation time constants and amplitudes have been measured for the five carriers (non, mon, din, trin, and tetranactin) at five NH_4^+ concentrations (10^{-3}, 10^{-2}, 10^{-1}, 0.5, and 1.0 M) and at four different voltages (10, 25, 50, and 100 mV). In each case we have seen only one time constant for the transient current (τ_{obs} and α_{obs}). In general, we have observed that at low voltage, as ion concentration is decreased, τ_{obs} and α_{obs} decrease and approach a finite limiting value, while as ion concentration is increased, α_{obs} increases linearly. Finally, at a given ion concentration, τ_{obs} strongly decreases with voltage while α_{obs} increases. Accordingly, as described by Hladky (1975; 1979a) as well as discussed by Stark et al. (1971) and Laprade et al. (1975; 1982), α_{obs} and τ_{obs} were identified with the slower relaxation process (α_1 and τ_1).

In all cases, our curve fitting procedure gave a good fit of

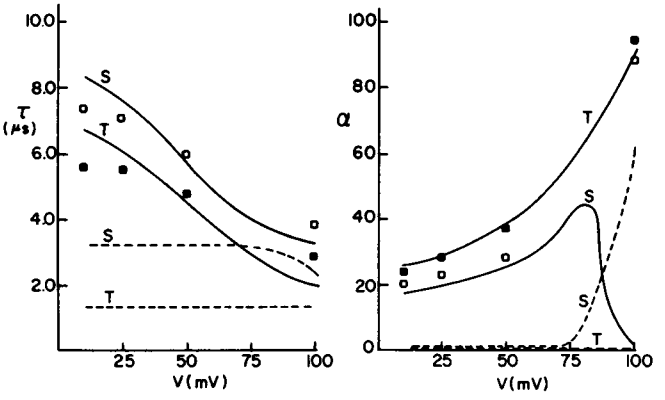

FIGURE 2 An example of curve fitting for the dinactin-NH_4^+ complex. The filled squares (■) represent the experimental data for GMO-T membrane; the open squares (□) are for GMO-S membrane. The solid curves represent theoretical curves corresponding to the best fit of τ_1 and α_1 to the experimental data using the values of Table II for the rate constants. The dashed curves represent the corresponding theoretical values of τ_2 and α_2. *S* and *T* refer to GMO-S and GMO-T membranes, respectively.

α_1 and τ_1 to α_{obs} at τ_{obs}, while the values of τ_2 and α_2 calculated with the optimal values of the parameters thus obtained confirm the fact that the second exponential was generally impossible to detect in our experimental conditions. Indeed, although the value of τ_2 might be in the same range as that of τ_1 (the ratio of τ_1/τ_2 varies between 1.5 and 5), the ratio α_2/α_1 is generally found to be $<10^{-2}$ except maybe at 100 mV where α_2 is sometimes comparable to α_1 (c.f. Fig. 2). However, in those few cases, we have discarded the corresponding values of α_{obs} (2 or 3 points over 40 τ_{obs} and α_{obs} for one carrier) in the final curve fitting program to avoid an unwanted constraint. Note that in these particular cases α_{obs} is close to $\alpha_1 + \alpha_2$ (c.f. Fig. 2). In contrast, if we try to fit τ_{obs} and α_{obs} with τ_2 and α_2, in all cases we find an unacceptable negative value at least for one of the rate constants. Therefore, we can be confident that the values of τ_{obs} and α_{obs} that have been used to obtain the values of the rate constants correspond indeed to τ_1 and α_1.

For the purpose of comparison, some experimental data at 1 M and 100 mV for GMO-D, GMO-S, and GMO-T

TABLE I
τ_{obs} AND α_{obs} FOR GMO-D, GMO-S, AND GMO-T MEMBRANES*

Carrier	Membrane	τ_{obs}	α_{obs}
		μs	
Nonactin	GMO-D	29	2.1
	GMO-S	5.7	16
	GMO-T	4.6	39
Tetranactin	GMO-D	12	58
	GMO-S	2.4	350
	GMO-T	1.8	1,200

*Values for NH_4^+ at 100 mV and 1 M.

are given in Table I. The standard deviation is approximately 15%. Before going into any theoretical interpretation, we can see that for all the carriers used, the solvent-free effect is primarily an increase of the relaxation amplitude and a decrease of the time constant (a factor ~10 for both). From Table I as well as for all our experimental τ_{obs} and α_{obs}, we can say that this effect is always more important for GMO-T than for GMO-S membranes.

Determination of the Rate Constants

In Table II we give the rate constants for each ion-carrier combination with the computer fit (see Numerical Methods) of the 40 experimental values of τ_{obs} and α_{obs} to the theoretical Eqs. 6 and 10. We give also the mean deviation of the experimental values from the theoretical curve in percent of the experimental values, [$\bar{\Delta}\% = 100\ (\Sigma|X_{exp} - X_{theor}|/X_{exp})/n$], where n is the number of points). This quantity has the advantage of being directly comparable to the expected incertitude for each point.

TABLE II
RATE CONSTANTS FOR GMO-D AND SOLVENT-FREE MEMBRANES

		GMO-D*	GMO-S	GMO-T
Nonactin	$k_{is}(s^{-1})$	2,800	35,000	45,000
	$k_s(s^{-1})$	86,000	140,000	180,000
	$k_{Ri}(M^{-1} - s^{-1})$	370,000	130,000	360,000
	$k_{Di}(s^{-1})$	32,000	21,000	21,000
	$k_{Ri}/k_s(M^{-1})$	4.30	0.93	2.00
	$\bar{\Delta}\%$	16.5	13.4	14.3
Monactin	k_{is}	5,100	50,000	53,000
	k_s	66,000	150,000	200,000
	k_{Ri}	170,000	150,000	280,000
	k_{Di}	20,000	12,000	10,000
	k_{Ri}/k_s	2.58	1.00	1.40
	$\bar{\Delta}\%$	13.6	12.9	14.0
Dinactin	k_{is}	7,700	56,000	74,000
	k_s	64,000	140,000	340,000
	k_{Ri}	320,000	250,000	630,000
	k_{Di}	13,000	7,400	6,100
	k_{Ri}/k_s	5.00	1.79	1.85
	$\bar{\Delta}\%$	15.0	12.1	14.1
Trinactin	k_{is}	9,000	63,000	78,000
	k_s	92,000	120,000	300,000
	k_{Ri}	170,000	270,000	130,000
	k_{Di}	9,000	7,000	5,200
	k_{Ri}/k_s	1.85	2.25	0.43
	$\bar{\Delta}\%$	16.8	11.0	14.5
Tetranactin	k_{is}	14,000	90,000	120,000
	k_s	61,000	220,000	200,000
	k_{Ri}	180,000	250,000	120,000
	k_{Di}	4,000	2,300	2,000
	k_{Ri}/k_s	2.95	1.14	0.60
	$\bar{\Delta}\%$	6.6	13.5	17.2

*Values from Laprade et al. (1982)

An example of curve fitting for dinactin with NH_4^+ at 0.1 M is given in Fig. 2. Generally the fit is quite acceptable because for all carriers the mean deviation is 14%, which is practically identical to our uncertainty for the experimental values. We see in Fig. 2 that the theory describes the experimental results adequately, although the voltage dependence of τ_{obs} appears to be too strong. However, the fit is good for intermediate voltages, and, although a better voltage dependence that improves the fit can be found, the values of the rate constants are not changed importantly; moreover, the relative variations from GMO-D to solvent-free membranes are virtually unchanged. Indeed, we have conducted a study based on Hladky's analysis (1975; 1979*a*; 1979*b*) that takes into account the actual voltage dependence of the rate constants as measured from the voltage dependence of τ_{obs} and a_{obs}, and allows the determination of the voltage-independent portion of k_{is}, k_{Di}, and k_{Ri}/k_s. The results show that, although the absolute values of k_{is} are then ~20% larger, and the values of k_{Di} are a factor of 2 smaller than those found in Table II even though there is little change in the values of k_{Ri}/k_s, the factors of increase or decrease of these parameters with membrane type are not significantly different from those obtained from Table II. Therefore, we can be confident that the observed solvent-free effects are not dependent on the voltage function used.

Reliability on the Values of Rate Constants

The values of the rate constants given in Table II correspond to the optimum fit, i.e., the least-square fit between the experimental values and the theoretically predicted ones. We will now try to evaluate the degree of reliability we can assign to these values. For this purpose, we assign a fixed value to one rate constant and let the curve fitting program find the values of the three remaining constants that give the best fit. We do this for values ranging from 10 times smaller to 10 times larger than the optimal value. For each value of the rate constant, we calculate the mean deviation, $\bar{\Delta}\%$, and plot it as a function of the ratio of the fixed value over the optimal one. This analysis has been performed for nonactin-NH_4^+ and tetranactin-NH_4^+ in GMO-S and GMO-T membranes (see Laprade et al., 1982, for GMO-D). The plots for different carriers and membranes are very similar and an example for nonactin and GMO-S is given in Fig. 3. Even though each parameter shows a minimum for the mean deviation, we can see that it is not as sharp for every one. k_{is} and k_{Di} are very well limited on both sides; k_{Ri}/k_s is more weakly limited, but also on both sides; k_s shows a small minimum with a clear indication of a lower limit; and k_{Ri} shows only a small influence on the quality of the fit, although a slight but definite minimum is seen.

The Solvent-free Effects

The most important results of this work are summarized in Fig. 4 where we compare, among the different homologues

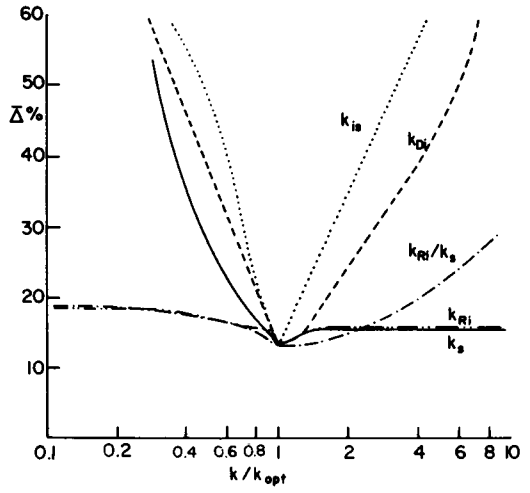

FIGURE 3 Illustration of the reliability on the values of the rate constants corresponding to the optimum fit for nonactin-NH_4^+ in GMO-S membranes. The value of a single rate constant is fixed at a value different from the optimal one, and the other three are allowed to vary to get a minimum in the mean relative error between predicted and experimental points ($\bar{\Delta}\%$). $\bar{\Delta}\%$ is plotted as a function of the ratio k/k_{opt} of the fixed over the optimal value.

of nonactin, the factor by which a given parameter increases or decreases from a GMO-D to a solvent-free membrane. We see that on the average, the solvent-free effects are, first of all, an increase in k_{is} by a factor of ~10, an increase in k_s by a factor of 2.5, a decrease in k_{Ri}/k_s by a factor of 3 and a decrease in k_{Di} by a factor of 1.5. In addition, we can state that all these effects are more pronounced for GMO-T than for GMO-S membranes. It is also very interesting to note that in Fig. 4, for both GMO-S and GMO-T, the increase in k_{is} with respect to GMO-D membranes becomes systematically less important with increasing methylation of the carrier.

The fact that the same behavior is seen for all homologues should be a good indication that these variations

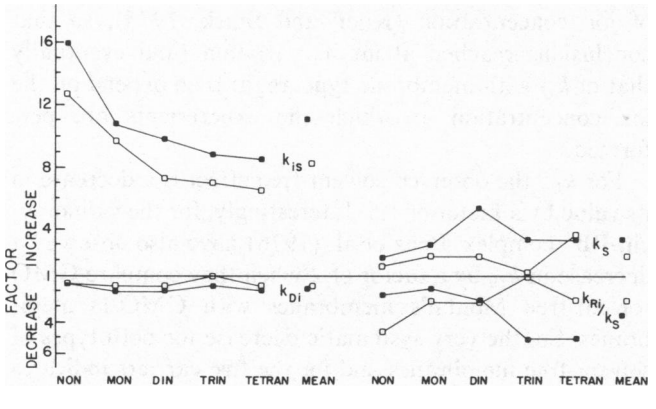

FIGURE 4 Factor of increase or decrease of the rate constants from GMO-D to solvent-free membranes. ■ and □ correspond to GMO-T and GMO-S membranes, respectively. Values of the rate constants from Table II. The mean factor for the five carriers appears on the right of each graph. Note that this mean factor is always higher for GMO-T than for GMO-S membranes.

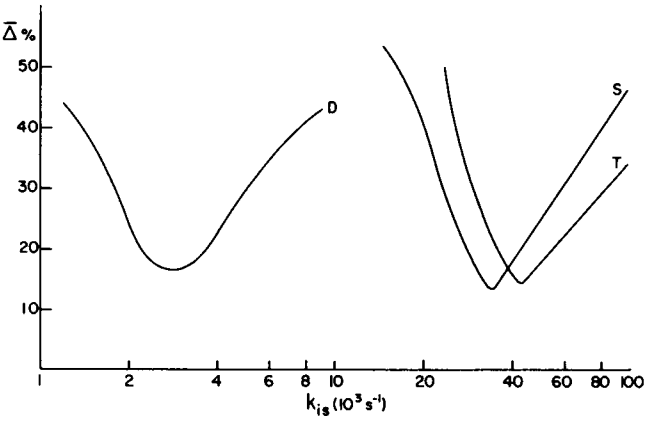

FIGURE 5 Reliability curves of k_{is} for nonactin-NH_4^+ in GMO-D, GMO-S, and GMO-T membranes. The curves have been drawn using the same method as in Fig. 3. For GMO-D membranes the data come from Laprade et al., 1982. We can see that the three optimum values of k_{is} are clearly differentiated even between the two solvent-free membranes.

from GMO-D to solvent-free membranes are real. However, the analysis of the reliability in terms of the mean deviation $\bar{\Delta}\%$, introduced above, allows further evaluation of the confidence in these variations.

If we consider first the rate constants k_{is} and k_{Di}, we have already seen (c.f. Fig. 3) that these parameters are very well defined. If we now refer to Figs. 5 and 6 we can see that there is absolutely no doubt that these two parameters have different values in GMO-D and solvent-free membranes because the minima in $\bar{\Delta}\%$ are very well separated. However, only for k_{is} could we claim a difference between GMO-S and GMO-T membranes because for k_{Di}, the minima are broader and overlap too much.

Fig. 3 shows that the minimum in $\bar{\Delta}\%$ for k_s as well as for k_{Ri}/k_s is less well defined than for k_{is} and k_{Di}. An even poorer definition is obtained for k_{Ri}. However, the fact that k_s is well limited on the lower end while k_{Ri}/k_s is limited on

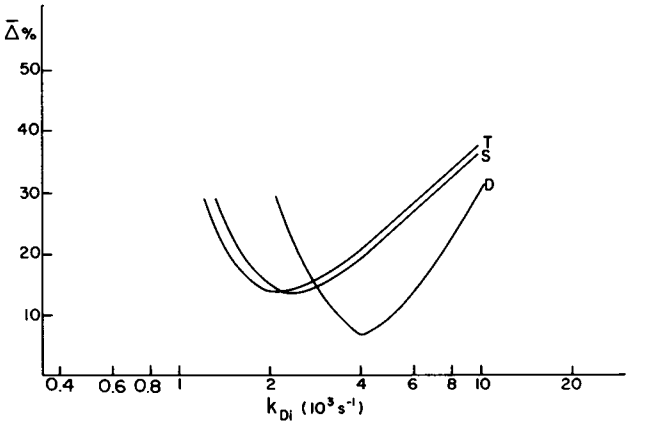

FIGURE 6 Reliability curves of k_{Di} for tetranactin-NH_4^+, this carrier being representative of the mean factor of decrease in k_{Di} (c.f. Fig. 4). The optimal values of k_{Di} are clearly different for solvent-free membranes and GMO-D membranes. However, we see no difference between the two solvent-free membranes.

both ends, together with the observation that k_{Ri} does not show any systematic trends from one type of membrane to the other allows us to suggest with some confidence that k_{Ri} is indeed rather invariant while k_s increases from GMO-D to solvent-free membranes. However, no variations between GMO-S and GMO-T membranes can be attributed with confidence to these parameters.

Determination of the Free Carrier Partition Coefficient γ_s

The aqueous phase-membrane free carrier partition coefficient can be obtained whether from the time constant, τ, for the establishment of the steady-state zero-conductance, G_o^a, after addition of the carrier to the aqueous phase and the beginning of stirring, or from the value of G_0^a in the low ion concentration limit, using Eq. 16 and the values of the appropriate rate constants from Table II. The expression for the partition coefficient in terms of τ (Hladky, 1973; Laprade et al., 1979) is given by

$$\gamma_s = \frac{C_s^*}{C_s} = \tau \frac{2D}{d\delta} \tag{17}$$

where $D = 3 \times 10^{-6}$ cm^2 $-$ s^{-1} is the carrier diffusion coefficient (Laprade et al., 1982), $\delta = 10^{-2}$ cm is the unstirred layer thickness (Hladky, 1973), and d is the membrane thickness, which is 22.6 Å for GMO-T and 24.8 Å for GMO-S membranes (White, 1978; Waldbillig and Szabo, 1979). The experimental values of τ and the calculated value of γ_s are respectively given in the third and fourth columns of Table III.

On the other hand, at low ion concentration the expression for the zero-current conductance, Eq. 16, becomes

$$G_0^a = \frac{F^2 d}{2RT} \frac{k_{is}}{k_{Di}} \gamma_s \frac{k_{Ri} c_s^a c_i}{1 + 2k_{is}/k_{Di}}. \tag{18}$$

Using Eq. 18, the values for the rate constants from Table II and those for G_o^a given in the fifth column, we find the results shown in the sixth column of Table III.

We can see that the agreement between the values of γ_s obtained with these two different methods is generally good within a factor of ~2. The reliability on the values of γ_s obtained with the help of Eq. 18 of course depends on the reliability on the values of the parameters k_{is}, k_{Di}, and k_{Ri}, the last being the most questionable one, as discussed above. Therefore the good general agreement between both sets of values of γ_s provides a good check on the values of k_{Ri} in Table II, which would then be reliable within a factor of ~2.

TABLE III
PARTITION COEFFICIENT γ_s

		τ	γ_s*	G_0^a	γ_s‡
	(s)			($\mu S - cm^{-2}$)	
Nonactin	GMO-S	110	2.7×10^5	56	2.4×10^5
	GMO-T	230	6.1×10^5	52	0.8×10^5
Tetranactin	GMO-S	320	7.7×10^5	210	3.6×10^5
	GMO-T	300	8.0×10^5	150	5.9×10^5

*Calculated with Eq. 17 and the values of τ.
‡Calculated with Eq. 18 and the values of G_0^a for NH_4^+ at $c_i = 10^{-3}$ M and $c_s^a = 10^{-8}$ M.

It is interesting to note that the above values of γ_s in solvent-free membranes are not significantly different from those found by Laprade et al. (1982) on GMO-D membranes. This would suggest, within the accuracy of the determination, that the absence of solvent in the bilayer does not significantly perturb the energy of the free carrier in the membrane near the interface.

DISCUSSION

Table II and Fig. 4 show for all carriers studied that solvent-free membranes have a higher k_s and a lower k_{Ri}/k_s ratio than GMO-D membranes. On the average for both GMO-S and GMO-T membranes, k_s increases by a factor of 2.5 while k_{Ri}/k_s decreases by a factor of 3. Interestingly, this increase in k_s is quite close to what is expected because (see Introduction) GMO solvent-free membranes are about two times thinner than GMO-D membranes. As for k_{Ri}/k_s, the major part of the observed decrease would then be already explained by this increase in k_s, which would argue in favor of negligible variations in the values of k_{Ri} as suggested above.

We might compare these findings on k_{Ri} and k_s with those of Benz et al. (1976) for the valinomycin-Rb^+ complex on GMO membranes. With solvent-free membranes made by the Montal's method (Montal and Mueller, 1972) as compared with GMO-D membranes, they observe, in agreement with our results, a decrease in the ratio k_{Ri}/k_s by a factor of 4. However, contrary to our findings, they find that it is k_{Ri} that decreases while k_s remains constant. However, this contradictory result might well be related to the peculiar behavior of valinomycin. Indeed, for this molecule, k_{Ri} is not a constant as a function of ion concentration (Knoll and Stark, 1975), so that conclusions reached about its variation (and eventually that of k_s) with membrane type might then depend on the ion concentration at which the experiments are performed.

For k_{Di}, the observed solvent-free effect is a decrease in its value by a factor of 1.5. Interestingly, for the valinomycin-Rb^+ complex, Benz et al. (1976) have also observed a decrease in k_{Di} by a factor of 2 when they compare GMO solvent-free Montal's membranes with GMO-D membranes. So, the very systematic decrease for both types of solvent-free membranes and for the five carriers indicates that the energy barrier height for dissociation has changed. Therefore, the solvent-free effect would not simply consist of a change of membrane thickness; the absence of solvent also seems to have changed something near the membrane interface. We will propose an explanation for this behavior in relation with the observed increase in k_{is}.

The most important solvent-free effect on carrier-mediated ion transport is undoubtedly the observed increase in k_{is} which is, in addition, carrier dependent. It seems that our results are intermediate between those of Benz et al. (1976) and those of Benz and Gisin (1978) where these authors compare the translocation rate constants of valinomycin-Rb^+, proline-valinomycin-K^+, and the lipophilic anion dipicrilamine (DPA^-) between GMO Montal's solvent-free and GMO-D membranes. For valinomycin, Benz et al. (1976) see an increase in k_{is} by only a factor of 1.5, and Benz and Gisin (1978) see no increase for proline-valinomycin and an increase by a factor 12 for DPA^-. It is interesting to note that valinomycin and proline-valinomycin, which have relatively large diameters (~15 Å), show little or no increase in k_{is} while DPA^-, which is smaller (16 × 8 × 4 Å from Corey-Pauling-Koltun space-filling [CPK] models), shows an important increase. Similarly for the actin homologues, for which the diameter decreases from tetranactin to nonactin (12.5 Å for nonactin), the corresponding increase in the value of k_{is} ranges from 6.5 to 12.5 (for GMO-S). (The above diameters for valinomycin and nonactin are taken from Simon and Morf, 1973.) It seems that the bigger the carrier is, the less it sees the solvent-free effect. We will discuss in the following section different possible explanations for this behavior of k_{is} in terms of electrostatic and hydrophobic energy profiles and would like to propose here that the carrier size influences the increase in k_{is} from GMO-D to solvent-free membranes.

Modifications of the Electrostatic Energy Barrier

Like previous authors (Benz et al., 1976; Benz and Gisin, 1978), we might first consider that the sole effect of the absence of solvent is a decrease of the electrostatic energy of the complex in the middle of the membrane, consequent to the decrease in membrane thickness. Therefore, the energy in units of kT for an ion at the center of a membrane of thickness d and dielectric constant ϵ_2 separating two aqueous phases of dielectric constant ϵ_1 (Parsegian, 1969; 1975) is given by

$$E_B(d/2) = E_{B\infty} - \frac{2q_o}{\epsilon_2 d} \ln \frac{2\epsilon_1}{\epsilon_1 + \epsilon_2} \qquad (19)$$

where $E_{B\infty}$ is the Born charging energy in an infinite medium, which, for a spherical carrier of radius r_c, is given by

$$E_{B\infty} = \frac{q_o}{\epsilon_2 r_c} + \frac{q_o}{\epsilon_c}\left(\frac{1}{r_i} - \frac{1}{r_c}\right), \qquad (20)$$

where ϵ_c and r_i are the carrier dielectric constant and the radius of the ion respectively, and

$$q_o = \frac{1}{4\pi\epsilon_o}\frac{e^2}{2kT} = 283 \text{ Å at } 22.5°C \qquad (21)$$

where ϵ_o is the free space permittivity constant and e, the elementary charge.

If the translocation rate constant is expressed as in the following equation:

$$k_{is} = (\text{constant}) \exp[-E_B(d/2)] \qquad (22)$$

we find for two membranes of thicknesses d' and d

$$\frac{k_{is}(d')}{k_{is}(d)} = \exp\left[\left(\frac{1}{d'} - \frac{1}{d}\right)\frac{2q_o}{\epsilon_2} \ln \frac{2\epsilon_1}{\epsilon_1 + \epsilon_2}\right]. \qquad (23)$$

For GMO-T, d' = 22.6 Å, for GMO-S, d' = 24.8 Å, and for GMO-D membranes, d = 49.5 Å. Using Eq. 23 with ϵ_1 = 78.5 and ϵ_2 = 2.2, we find that k_{is} should increase by a factor of 32 for GMO-S, and by a factor of 62 for GMO-T membranes. Consequently, the variation of the energy level at the top of the energy barrier predicts an increase in k_{is} in the right direction although much larger than observed (32 instead of 8 for GMO-S and 62 instead of 11 for GMO-T). Taking into account the influence of thickness on the electrostatic energy of the complex near the interface (Neumcke and Läuger, 1969), which would then imply a less reduced barrier height from GMO-D to solvent-free membranes, does not improve the agreement satisfactorily because the complex would have to sit in the middle of the membrane in order to reconcile quantitatively the results with the above hypothesis. In addition, this hypothesis does not explain why the increase in k_{is} from GMO-D to solvent-free membranes is a function of carrier methylation or size. In the following, we will therefore consider other factors that might modulate this increase in k_{is}.

Variation of the Position of the Adsorption Distance with Carrier Size and Membrane Thickness

We have shown in a previous paper (Laprade et al., 1982) that we could explain the increase of k_{is} with increasing carrier methylation by considering that due to its larger size, a larger complex would be adsorbed with its center further away from the interface. Not only could we show that this hypothesis was compatible with the observed increase in k_{is} with methylation, but also that it could explain the concomitant decrease in k_{Di}, as well as predict the observed relationship between these two constants. In this approach, we had used the following expression deduced by Neumcke and Läuger (1969) for the energy near the interface.[1]

[1]This expression assumes that the complex is considered to be in a semi-infinite medium and thus neglects the image forces of the second interface. This assumption is well justified in the cases that will be studied here where h is small compared to the membrane thickness. Moreover, Eq. 24 will be used solely to compare carriers and because in this comparison only differences in $E_B(h)$ will be considered, the eventual small correction will practically vanish.

$$E_B(h) = E_{B\infty} - \frac{\nu q_o}{2\epsilon_2 h} \quad (24)$$

where h, is the adsorption distance and corresponds to the distance of the center of the complex (ion) from the interface, and

$$\nu = (\epsilon_1 - \epsilon_2)/(\epsilon_1 + \epsilon_2). \quad (25)$$

Consequently, the barrier height seen by a complex will correspond to the difference between the electrostatic energy in the middle of the membrane and that at the adsorption site near the interface, and therefore to the difference between Eqs. 19 and 24

$$\Delta E_B = -\frac{q_o}{\epsilon_2}\left[\frac{2}{d}\ln\frac{2\epsilon_1}{\epsilon_1 + \epsilon_2} - \frac{\nu}{2h}\right]. \quad (26)$$

Accordingly, if we compare in the same type of membrane, k_{is} for two different complexes of the same ion with respective adsorption distances, h_1 and h_2, we find

$$\frac{k_{is}^1}{k_{is}^2} = \exp\left[\frac{\nu q_o}{2\epsilon_2}\left(\frac{1}{h_2} - \frac{1}{h_1}\right)\right]. \quad (27)$$

If we assume that the complex is adsorbed such that its edge more or less coincides with the interface in GMO-D membrane (i.e., $h \simeq r_c$, where r_c is the radius of the complexes) and take 6.3 Å for the radius of the nonactin complex (Simon and Morf, 1973), with the help of Eq. 27 and the observed values of k_{is} from Table II we can calculate the values for the adsorption distances (complex radii) for the other homologues. These values for GMO-D membranes appear in the second row of Table IV.[2] We see, within the present framework where the adsorption distance is related to the carrier size, that the average tetranactin complex radius in GMO-D membranes would be 7.6 Å, i.e., 1.3 Å larger than nonactin. This result is quite reasonable because tetranactin has four additional methyl groups compared with nonactin, which are distributed symmetrically and whose diameters are 1.54 Å (twice the covalent radius of a CPK model of a tetrahedral carbon).

TABLE IV
CALCULATED ADSORPTION DISTANCE (Å)

	GMO-D	GMO-S	GMO-T
Nonactin	6.30*	5.75	5.53
Monactin	6.72	5.96	5.62
Dinactin	7.04	6.02	5.80
Trinactin	7.18	6.09	5.83
Tetranactin	7.56	6.32	6.07

*Assumed from Simon and Morf (1973)

[2]An identical calculation has been performed by Laprade et al. (1982), although very slightly different values were obtained due to the use of $\epsilon_2 = 2$ instead of 2.2.

On the other hand, if we compare k_{is} for a given ion-carrier complex in two different types of membrane and allow, in addition, the position of the adsorption site to vary from one membrane type to the other, we find

$$\frac{k_{is}(d_1)}{k_{is}(d_2)} = \exp\frac{q_o}{\epsilon_2}\left[2\left(\frac{1}{d_1} - \frac{1}{d_2}\right)\ln\frac{2\epsilon_1}{\epsilon_1 + \epsilon_2} - \frac{\nu}{2}\left(\frac{1}{h_1} - \frac{1}{h_2}\right)\right] \quad (28)$$

where h_1 and h_2 then correspond to the adsorption distances in the membranes of thickness d_1 and d_2, respectively. That a given ion-carrier complex may not be adsorbed at the same distance from the interface in two different types of membrane would be consistent with our finding that something has changed near the interface, as suggested by the variations of k_{Di} with membrane type. Then, using the values in Eq. 28 for h_2 deduced for GMO-D membranes, together with the known values of the membrane thickness (c.f. Introduction) and the observed increase in k_{is} from GMO-D to solvent-free membranes (Table II), we obtain the adsorption distances for the different homologues, given in the last two rows of Table IV.

We see that for the solvent-free membranes, the adsorption distance, on the average, would be only 1 Å smaller than that for GMO-D membranes. In addition, we see that for these thinner membranes the decrease in the adsorption distance would be more pronounced for the larger carriers, as if the latter were pushed out to a greater extent.

First of all, it is important to emphasize that a decrease as small as 1 Å in the adsorption distance is sufficient to reconcile with the theory the observed increases in k_{is} from GMO-D to solvent-free membranes. Moreover, a decrease in the adsorption distance is quite reasonable if one considers that in these thin, solvent-free membranes the carrier spans slightly more than half the membrane dielectric thickness for the smaller homologues and would tend to overlap the center of the membrane for the larger ones. In this context, it might well be that the lipid molecules in the center of the membrane that are bent and more or less running parallel to the plane of the bilayer (White, 1977) would tend to prevent the carrier edge from going further than the middle of the membrane, and thus push it towards the interface. We would then expect the adsorption distance in solvent-free membranes, with respect to GMO-D membranes, to decrease more for the larger homologues as well as for the thinner membranes; this is in perfect agreement with what is observed.

Therefore, the above hypothesis where carrier size and membrane thickness modulate the adsorption distance of the complex would not only be useful to explain our results with the nonactin homologues but might furnish at least part of the explanation for the invariance in k_{is} as a function of membrane thickness described above for the valinomycin homologues that have a much larger size.

This variation in the adsorption distance from GMO-D to solvent-free membranes that allows us to explain the

observed variations in k_{is} between these two types of membranes should, however, influence the rate of dissociation k_{Di} because this rate depends on the ion energy level at the interface. Indeed, if we refer to Fig. 7 where we show for a given carrier the ion energy profiles for two different membrane thicknesses, we see that k_{Di} depends on the level of the energy minimum near the interface as well as the height of the energy maximum for the complexation reaction. One does not expect this energy maximum for complexation to change very much from one membrane type to the other because we have seen no systematic variations in k_{Ri} (c.f. Table II). Therefore, if we assume that the variations in k_{Di} are mostly determined by the variations in the energy minimum of the complex near the interface, we predict that a thinner membrane should give a smaller value of k_{Di} because its energy minimum is lower due to its smaller adsorption distance. Interestingly, it can be seen in Table II that the predicted variations are indeed in the right direction.

Finally, we might add that, obviously, other factors besides the image-force electrostatic energy might influence the energy level of the complex within the membrane. For example, if the dielectric constant for these three types of membranes were higher than the postulated value of 2.2, or better, if the dielectric constant of the solvent-free membranes were higher than that of GMO-D membranes, the discrepency between the observed increase in k_{is} and that predicted solely from the change in the energy level in the middle of the membrane would be smaller, so that smaller variations in the adsorption distances would be needed in the treatment above. We must also realize that we have always assumed in the present discussion that decane only influences the membrane thickness and behaves exactly like the hydrocarbon chains of the lipid molecules. Indeed, it is interesting to recall here that in GMO-D membranes, the decane is not distributed uniformly across the width of the membrane but concentrated in the center of the membrane (McIntosh et al., 1980). Therefore, the possible variation in fluidity induced by the change from extended to bent configuration of the lipid molecules, as well as the possible variation in the hydrophobic energy profile due to the absence of solvent, might also influence the translocation rate constant of the complex.

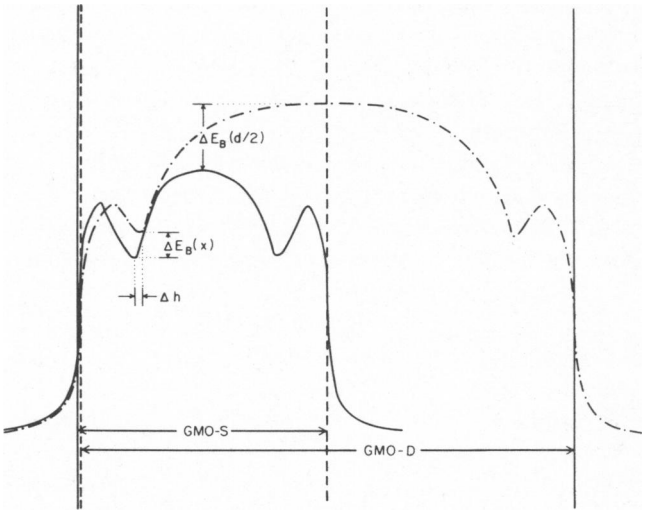

FIGURE 7 Electrostatic energy barriers for an ion crossing two different membranes with the same carrier. The energy profiles have been approximated with the help of Eqs. 19, 20, and 24, assuming r_c = 6.3 Å, $\epsilon_c > 10$, and the usual values for the other parameters. If we compare a GMO-S to a GMO-D membrane, we have $\Delta E_B(d/2)$ = 3.44 kT so that $\Delta E_B(x)$, due to a change in adsorption distance Δh, has to be between 0.9 and 1.6 kT to explain the factor of increase observed for k_{is} with our five carriers. The corresponding displacement Δh, would then be between 0.5 and 1.3 Å.

We would like to express our gratitude to G. Szabo, R.C. Waldbillig, and S.H. White for the details on formation of solvent-free bilayers. We also gratefully acknowledge Dr. K. Ando and Dr. W. Simon for the gifts of tetranactin and Dr. Hans Bickel and Ms. Barbara Stearns for the gifts of nonactin, monactin, dinactin, and trinactin. Finally, we are very grateful to Ms. Louise Lefort for her competent and dedicated secretarial work.

This work was supported by the CRSNG grant A9598 Canada and by the FCAC grant EQ0904 Quebec.

Received for publication 16 June 1981 and in revised form 8 December 1981.

REFERENCES

Benz, R., O. Fröhlich, P. Läuger, and M. Montal. 1975. Electrical capacity of black lipid films and of lipid bilayers made from monolayers. *Biochim. Biophys. Acta.* 394:323–334.

Benz, R., O. Fröhlich, and P. Läuger. 1976. Influence of membrane structure on the kinetics of carrier mediated ion transport through lipid bilayers. *Biochim. Biophys. Acta.* 464:465–481.

Benz, R., and B. F. Gisin. 1978. Influence of membrane structure on ion transport through lipid bilayer membranes. *J. Membr. Biol.* 40:293–314.

Ciani, S. M., G. Eisenman, R. Laprade, and G. Szabo. 1973. Theoretical analysis of carrier-mediated electrical properties of bilayer membranes. *In* Membranes—A Series of Advances. G. Eisenman, editor. Marcel Dekker, Inc., New York. 2:61–177.

Fettiplace, R., D. M. Andrews, and D. A. Haydon. 1971. The thickness, composition, and structure of some lipid bilayers and natural membranes. *J. Membr. Biol.* 5:277–296.

Henn, F. A., and T. E. Thompson. 1968. Properties of lipid bilayer membranes separating two aqueous phases: composition studies. *J. Mol. Biol.* 31:227–235.

Hladky, S. B. 1973. The effect of stirring on the flux of carriers into black lipid membranes. *Biochim. Biophys. Acta.* 307:261–269.

Hladky, S. B. 1975. Tests of the carrier model for ion transport by nonactin and trinactin. *Biochim. Biophys. Acta.* 375:327–344.

Hladky, S. B. 1979*a*. The carrier mechanism. *In* Current Topics in Membranes and Transport. Academic Press, Inc., New York. 12:53–164.

Hladky, S. B. 1979*b*. Ion transport and displacement currents with membrane-bound carriers. *J. Membr. Biol.* 46:213–237.

Knoll, W., and G. Stark. 1975. An extended kinetic analysis of valinomycin-induced Rb-transport through monoglyceride membranes. *J. Membr.* Biol. 25:249–270.

Laprade, R., S. M. Ciani, G. Eisenman, and G. Szabo. 1975. The kinetics of carrier mediated ion permeation in lipid bilayers and its theoretical interpretation. *In* Membranes—A Series of Advances. G. Eisenman, editor. Marcel Dekker, Inc., New York. 3:127–214.

Laprade, R., F. Grenier, and S. Asselin. 1979. Measurement of lateral

diffusion coefficient of ion carriers in lipid bilayers using conductance measurements. *Biophys. J.* (*Abstr.*) 25:180*a*.

Laprade, R., F. Grenier, J. Y. Lapointe, and S. Asselin. 1982. Effects of variation of ion and methylation of carrier on the rate constants of macrotetralide-mediated ion transport in lipid bilayers. *J. Membr. Biol.* In press.

Läuger, P., and G. Stark, 1970. Kinetics of carrier-mediated ion transport across lipid bilayer membranes. *Biochim. Biophys. Acta.* 211:458–466.

McIntosh, T. J., S. A. Simon, and R. C. MacDonald. 1980. The organization of *n*-Alkanes in lipid bilayers. *Biochim. Biophys. Acta.* 597:445–463.

Montal, M., and P. Mueller, 1972. Formation of bimolecular membranes from lipid monolayers and a study of their electrical properties. *Proc. Natl. Acad. Sci. U. S. A.* 69:3561–3566.

Mueller, P., D. O. Rudin, H. T. Tien, and W. C. Wescott. 1962. Reconstitution of cell membrane structure in vitro and its transformation into an excitable system. *Nature* (*Lond.*). 194:979–980.

Neumcke, B., P. Läuger. 1969. Nonlinear electrical effects in lipid bilayer membranes. II. Integration of the generalized Nernst-Planck equations. *Biophys. J.* 9:1160–1170.

Pagano, R. E., J. M. Ruysschaert, and I. R. Miller. 1972. The molecular composition of some lipid bilayer membranes in aqueous solutions. *J. Membr. Biol.* 10:11–30.

Parsegian, A. 1969. Energy of an ion crossing a low dielectric membrane: solutions to four relevant electrostatic problems. *Nature* (*Lond.*). 221:844–846.

Parsegian, A. 1975. Ion membrane interactions as structural forces. *Ann. N.Y. Acad. Sci.* 264:161–174.

Simon, W., and W. E. Morf. 1973. Alkali cation specificity of carrier antibiotics and their behavior in bulk membranes. *In* Membranes—A Series of Advances. G. Eisenman, editor. Marcel Dekker, Inc., New York. 2:329–375.

Stark, G., B. Ketterer, R. Benz, and P. Läuger. 1971. The rate constants of valinomycin-mediated ion transport through thin lipid membranes. *Biophys. J.* 11:981–994.

Szabo, G., G. Eisenman, and S. Ciani, 1969. The effects of the macrotetralide actin antibiotics on the electrical properties of phospholipid bilayer membranes *J. Membr. Biol.* 1:346–382.

Waldbillig, R. C., and G. Szabo. 1978. Solvent depleted bilayer membranes from concentrated lipid solutions. *Nature* (*Lond.*). 272:839–840.

Waldbillig, R. C., and G. Szabo. 1979. Planar bilayer membranes from pure lipids. *Biochim. Biophys. Acta.* 557:295–305.

White, S. H., D. C. Petersen, S. Simon and M. Yafuso. 1976. Formation of planar bilayer membranes from lipid monolayers. A critique. *Biophys. J.* 16:481–489.

White, S. H. 1977. Studies of the physical chemistry of planar bilayer membranes using high-precision measurements of specific capacitance. *Ann. N.Y. Acad. Sci.* 303:243.

White, S. H. 1978. Formation of "solvent-free" black lipid bilayer membranes glyceryl monooleate dispersed in squalene. *Biophys. J.* 23:337–347.